


Zihim Lam*
Harald Anlauf
Hermann Nirschl

High-Pressure Jet Cleaning of Polymeric Microfiltration Membranes

The cleaning effect of a high-pressure jet of water on a polymeric microfiltration membrane was investigated at different pressures, durations, and angles. The angle of 70° at a pressure of 130 bar and a cleaning duration of 10 s were found to be promising parameters. Throughput measurements show that this cleaning method can restore about 80 % of the initial throughput of the membrane. Analyses by capillary flow porometer and UV-vis spectrophotometer imply that an impact on the membrane was detectable after 1800 cleaning cycles at a pressure of 130 bar. Therefore, high-pressure jet cleaning is a promising method for mechanical cleaning of track-etched microfiltration membranes.

 This is an open access article under the terms of the Creative Commons Attribution License, which permits use, distribution and reproduction in any medium, provided the original work is properly cited.

Keywords: High-pressure cleaning, Mechanical cleaning, Membrane cleaning, Microfiltration membranes

Received: August 14, 2019; *revised:* October 06, 2019; *accepted:* December 17, 2019

DOI: 10.1002/ceat.201900449

1 Introduction

Membranes are widely used for separation processes in the beverages, food, and pharmaceutical fields. However, the application of membranes is limited by their high cost of operation and maintenance. One major problem in membrane filtration is fouling. Based on the attachment strength of the fouling materials, four types of fouling can be defined: reversible, irreversible, residual, and irrecoverable fouling [1]. In the case of reversible fouling, a cake layer is deposited on the surface of the membrane, with loose attachment of the fouling material [2]. Irreversible fouling is caused by the formation of a strong matrix or a gel layer during continuous filtration, which cannot be further removed by physical cleaning [1, 3, 4]. Residual fouling can be removed by recovery cleaning. When the original flux of the membrane cannot be restored by the typical cleaning methods, one speaks of irrecoverable fouling [5, 6].

In general, the cleaning methods are categorized into physical, chemical, and biological cleaning. For the chemical cleaning, different chemicals can be used to either reduce or increase the pH, resulting in a lower interaction between the fouling substance and the membrane. Biological cleaning is the use of bioactive agents to remove membrane foulants. Physical cleaning is widely achieved by hydraulic, mechanical, and ultrasonic processes to remove the reversible fouling layers.

Recently, many researchers have used ultrasound to clean fouled membranes or even control membrane fouling [7–11]. During ultrasonic cleaning, microjets are formed above the surface of the membrane, with an average velocity of 100–200 m s⁻¹ [12]. These strong jets can cause damage to the membrane, resulting in membrane erosion. Various studies show the influence of ultrasound on membrane erosion [13–16]. Especially the power level of ultrasonic cleaning and the membrane material determine the level of membrane

erosion [13, 16]. Juang and Lin [16] showed that a horn transducer at a distance of 10 mm with more than 80 W power destroyed the membrane. Masselin et al. [13] observed that a polyethersulfone membrane was damaged by ultrasonic cleaning and showed large holes across the membrane surface.

A new method to clean the flat sheet membranes in an effective way is the use of a high-pressure jet. The high-pressure cleaning jet offers new possibilities to clean membranes in a continuous way. Cleaning membranes from the filtration side without submerging the membrane allows the development of new membrane filtration devices or the implementation of membranes in commonly used filtration devices. For example, the high-pressure cleaning jet can be used for the novel thin-film filtration process where the membrane is installed on a vacuum drum filter [17, 18]. On a vacuum drum filter, the backwash is a commonly used procedure to clean the filter cloths. However, the thin-film filtration on a vacuum drum filter is realized using membranes. The backwash of these membranes on a vacuum drum filter would need additional support on the filtrate side to stabilize the membrane during this cleaning procedure [19]. The novel thin-film filtration uses a roller discharge to remove the pasty filter cake. This mechanical support would affect the roller discharge of the thin filter cake. The high-pressure cleaner can be placed in front of the vacuum drum filter (Fig. 1). During the cleaning process, a drainage channel can be used to catch the washing liquid, preventing contamination of the suspension with the washing liquid.

Zihim Lam, Dr.-Ing. Harald Anlauf, Prof. Dr.-Ing. Hermann Nirschl,
zihim.lam@kit.edu

Karlsruhe Institute of Technology, Institute of Mechanical Process Engineering and Mechanics, Straße am Forum 8, 76131 Karlsruhe, Germany.

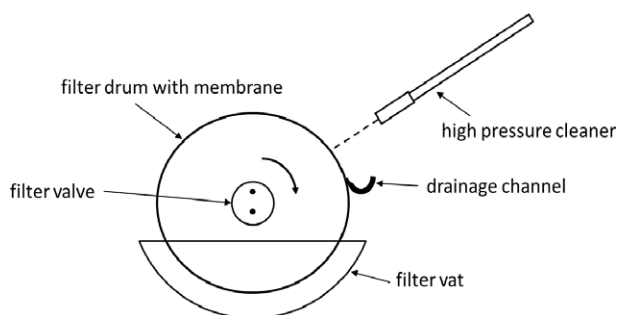


Figure 1. Vacuum drum filter during the cleaning process using the high-pressure jet cleaner.

This paper investigates the cleaning effect of the high-pressure jet at different pressures, cleaning durations, and angles, using polymeric microfiltration membranes. First, the effect of the high-pressure jet on the polymeric membranes is investigated. The pore size distribution of the membrane after 10 times of cleaning is analyzed in a capillary flow porometer and compared to the pore size distribution of a new membrane. This gives evidence of whether high-pressure cleaning changes the morphology of the membrane.

In the further steps, the membranes were fouled in a laboratory filter cell with a microalgae suspension. The fouled membranes were then cleaned using different operating parameters. After high-pressure jet cleaning, the throughput and the pore size distribution of the membranes were compared to each other and discussed. Additionally the filtrate was analyzed in a UV-vis spectrophotometer to determine the retention of microalgae particles. Based on the retention rate of the membrane, the impact of the high-pressure cleaning, and therefore the mechanical influence of the high-pressure cleaning, on the membrane can be quantified.

2 Materials and Methods

2.1 Sample Preparation

The microalgae *Nannochloropsis salina* were used for all fouling experiments (BlueBioTech GmbH, Büsum, Germany). The microalgae suspension was received from BlueBioTech immediately after cultivation. The microalgae were cultivated in photobioreactors and did not exceed 1 week for the experiments. It is assumed that extracellular and intracellular polymeric substances as well as dissolved organic matters of the microalgae caused the fouling effect. The concentrated microalgae suspension was received at a dry mass of 11.0 wt % and a mean particle size of $x_{50,3} = 2.8 \mu\text{m}$.¹⁾ The particle size was measured by laser diffraction (HELOS/Quixel; Sympatec GmbH, Germany). The pH of 6.8 was measured using a pH meter at a temperature of 20 °C (WTW pH 3310; Xylem Analytics Germany GmbH, Weilheim, Germany). The microalgae suspension was dried in an oven for 24 h at a temperature of 90 °C to determine the dry

mass. After receiving the concentrated suspension from the manufacturer, the suspension was diluted to a dry mass of 2.0 wt % with a 3.0-wt % NaCl solution.

The track-etched flat sheet membranes with supporting fibers used are made of polyethylene terephthalate (PET) and have an average pore size distribution of 1.1 μm (RoTrac 1.0; Oxyphen AG, Wetzikon, Switzerland). Prior to filtration in the laboratory filter cell, the membranes were submerged in 200 mL Milli-Q water for 10 min to moisten the hydrophilic membrane. The pictures of the membranes were captured by scanning electron microscopy (SEM) (S-4500; Hitachi, Japan). The image slice of the membrane was obtained by computed tomography (CT) (Xradia 520 Versa; Zeiss, Germany). For the analysis of the filtrate, a UV-vis spectrophotometer was used (Genova, Jenway, UK). The UV-vis analysis of the microalgae was performed at a wavelength of 550 nm.

2.2 Experimental Setup

2.2.1 Fouling and Cleaning of the Membrane

For the fouling experiments and the throughput measurements, a cylindrical laboratory filter cell with a diameter of 5 cm and a resulting filter area of $A = 19.63 \text{ cm}^2$ was used. The filter cake was formed at a pressure difference of $\Delta p = 0.8 \text{ bar}$. The specific liquid throughput TP is calculated from the volume flow rate Q , the gas differential pressure Δp and the filter area A (Eq. 1).

$$TP = \frac{Q}{A \Delta p} \quad (1)$$

The relative throughput TP_{rel} refers to the throughput of a new membrane TP_0 and is described by Eq. (2).

$$TP_{\text{rel}} = \frac{TP}{TP_0} \times 100\% \quad (2)$$

The new membrane has an average throughput of $TP_0 = 132160 \text{ L h}^{-1} \text{ m}^{-2} \text{ bar}^{-1}$. The high-pressure cleaning experiments were conducted on the device shown in Fig. 2. The high-pressure cleaning device with a flat nozzle spray angle of 25° was used for all cleaning experiments (HD 6/15; Kärcher GmbH, Germany). The pressure of the jet at $p = 30 \text{ bar}$ or $p = 130 \text{ bar}$ was adjusted by a throttle valve and the jet had a mass flow of 4.2 or 8.6 kg min^{-1} , respectively. This results in velocities of $v_{30} = 2.9 \text{ m s}^{-1}$ and $v_{130} = 5.95 \text{ m s}^{-1}$. Water with an electrical conductivity of 661 $\mu\text{S cm}^{-1}$ was used for all cleaning experiments. The nozzle was pointed at the membrane at a distance of $d = 50 \text{ cm}$. The membrane was fixed on an adjustable stand. With this adjustable stand, the angles of $\alpha = 15^\circ$, 70° , and 90° for each set of experiments can be set. The cleaning duration t was controlled by the rotation speed of the spray lance with an electric motor (940DC; RS PRO, Germany), which is connected to a power supply (DC 6005D; Peak Tech, Germany). The spray lance moves from the right side to the left side of the membrane with a speed of $v = 5 \text{ cm s}^{-1}$ or $v = 10 \text{ cm s}^{-1}$, resulting in a cleaning duration of $t = 10 \text{ s}$ or $t = 5 \text{ s}$, respectively.

1) List of symbols at the end of the paper.

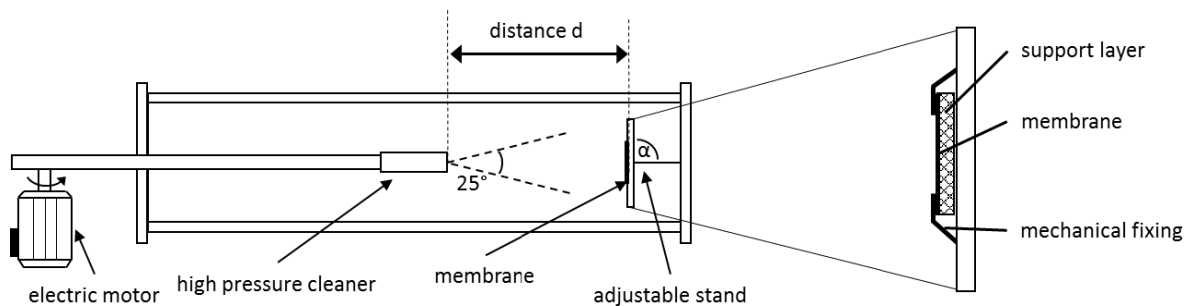


Figure 2. High-pressure cleaning device with an adjustable angle α , the distance d , and an electric motor to control the cleaning duration t .

2.3 Experimental Procedure

2.3.1 Membrane Fouling

Fouling of the membrane and the measurements of the throughput were carried out at a pressure of $\Delta p = 0.8$ bar. At each filtration step, 5 mL of the 2-wt % microalgae suspension was filtered in a dead-end filtration mode. After filtration, the formed filter cake was gently removed by immersion of the membrane in a water bath with Milli-Q water at room temperature. This filtration procedure was repeated 20 times before the membrane was cleaned and the throughput of the membrane was measured in the laboratory filter cell. The throughput TP is measured before and after the cleaning process to evaluate the cleaning effect. After 200 filtration cycles and 10 cleaning cycles, the pore size distribution of the membranes was analyzed in a capillary flow porometer (Porous Materials Inc., Ithaca, NY, USA). The evaluation of the pore size distribution can reveal damages resulting in larger pores, caused by the high-pressure cleaning jet.

3 Results and Discussion

At first, the throughput of the fouled membrane without any cleaning was analyzed. The membrane shows a decreased throughput due to fouling. As can be seen in Fig. 3, the throughput is gradually lowered to about 7% of the initial throughput after 200 filtration steps. After 20 filtration steps, the throughput drops to about 50% of the original throughput.

The SEM images in Fig. 4 visualize a new membrane and a membrane covered with fouling substances on the surface and in the pores. The arrows on the right side in Fig. 4 point at the fouling substances that block the pores. After 20 times of filtration, only about half of the initial throughput remains. Fouling substances that are located further inside the membrane cannot be displayed in the SEM images. However, the fouling layer that is on the surface of the membrane and foulants

within the membrane contribute to the decreased throughput of the membranes and may explain the drastic reduction of the throughput.

In the next step, the pore size distributions of the membrane before and after cleaning were compared. At first, 10 times cleaning was performed without fouling, to emphasize the possible impact of the high-pressure jet cleaning on the membrane. Then, the cleaning cycles were increased to 1800.

The pore size distributions before and after high-pressure cleaning do not differ significantly (Fig. 5a). The mean pore diameter of the cleaned membrane ($x_{m10} = 1.17 \pm 0.02 \mu\text{m}$) is

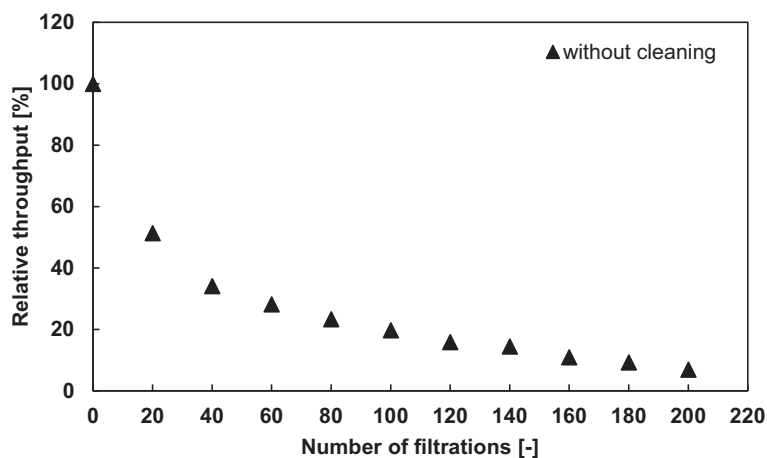


Figure 3. Influence of fouling on the throughput of the membrane after 200 filtration steps at $\Delta p = 0.8$ bar.

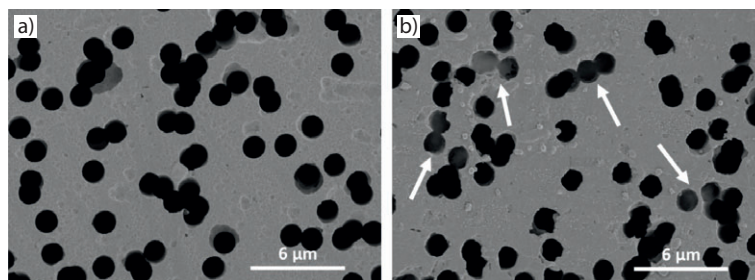


Figure 4. SEM images of the membranes. (a) New membrane without fouling. (b) Membrane after 200 times of filtration with a 2-wt % microalgae suspension; the fouling is visible in the pores.

only slightly larger than the mean pore diameter of the new one ($x_m = 1.10 \pm 0.02 \mu\text{m}$).

Even after 1800 times of cleaning the membrane has a similar mean pore diameter of $x_{m1800} = 1.16 \pm 0.02 \mu\text{m}$. However, some larger pores with a diameter of around $13 \mu\text{m}$ can be seen in the pore size distribution in the set of experiments performed at 130 bar pressure (Fig. 5b). Therefore, some damage could be detected at a pressure of $p = 130 \text{ bar}$ after 1800 cleaning cycles. This validation can explain the measurements in the UV-vis spectrophotometer, where traces of microalgae were found in the filtrate after 1800 cleaning cycles and at the cleaning pressure of 130 bar (Fig. 6). A dry mass of 0.01 % microalgae was found in the filtrate. As a result, it can be assumed that this cleaning method will only slightly affect the membrane below 1800 cleaning cycles. The filtrate of the membranes cleaned at pressures of 30 and 80 bar did not show traces of microalgae after 1800 times of cleaning. In this study, the dry mass of 0.01 % in the filtrate was set as a damage criterion.

Fig. 7 shows that only very thin walls between the pore channels were affected. This explains the minor increase of the larger pore size after the cleaning procedure. The majority of the pore channels that are surrounded by more membrane material remain unharmed by the high-pressure jet cleaning. Therefore, these membranes show a good mechanical stability towards the high-pressure jet cleaning.

In the following steps, the influence of the different operation parameters on the high-pressure cleaning jet will be presented.

3.1 Influence of the Pressure

After fouling in the laboratory filter cell, the membranes were cleaned at a pressure of $p = 30 \text{ bar}$ and $p = 130 \text{ bar}$. The two sets of experiments were carried out at an angle of $\alpha = 90^\circ$, a duration of $t = 5 \text{ s}$, and a distance of $d = 50 \text{ cm}$. Fig. 8a compares the different throughputs between the cleaning cycles at $p = 30 \text{ bar}$ and $p = 130 \text{ bar}$. The throughput of the membrane after cleaning at $p = 30 \text{ bar}$ can only be restored to up to 60 % of the initial value. The throughput after each cleaning cycle at 30 bar shows a distinctive decline. Foulants that got into the deeper structure of the membrane cannot be removed by the high-pressure jet and accumulate during filtration. The foulants reduce the size of the pores and can even clog them. As a result, the initial throughput of the membrane cannot be fully recovered. These remaining foulants are considered as residual fouling and cannot be effectively removed by mechanical cleaning methods.

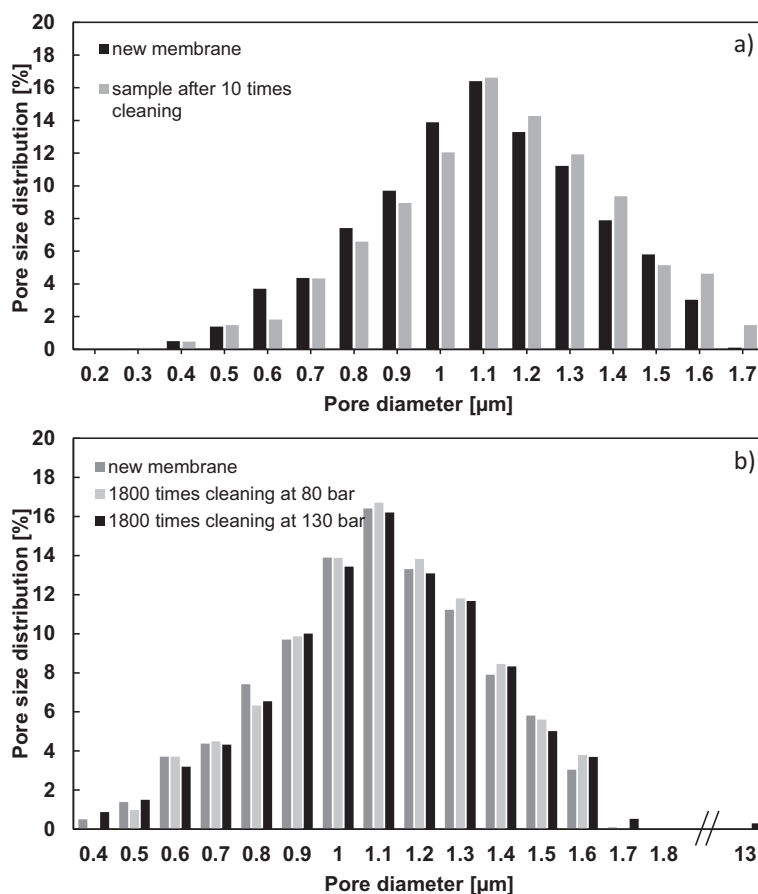


Figure 5. (a) Pore size distribution of the membrane before and after 10 times of cleaning with the high-pressure jet. (b) Pore size distribution of the membrane before and after 1800 times of cleaning with the high-pressure jet ($d = 50 \text{ cm}$, $\alpha = 90^\circ$, $p = 30 \text{ bar}$, $t = 5 \text{ s}$). A capillary flow porometer was used for the measurement.

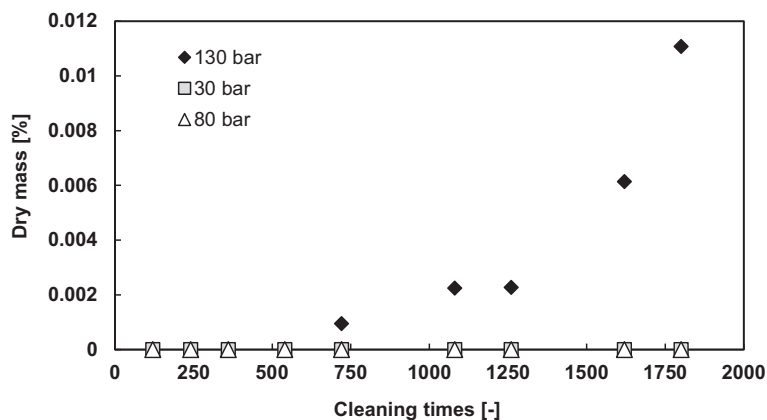


Figure 6. Analyses by UV-vis spectrophotometer reveal the dry mass of microalgae in the filtrate. A dry mass of 0.01 % was found in the filtrate after 1800 times of cleaning.

Meng et al. [20] and Kraume et al. [21] describe, for cross-flow filtration, that the accumulation and the detachment are defined by the particle convection towards the membrane and

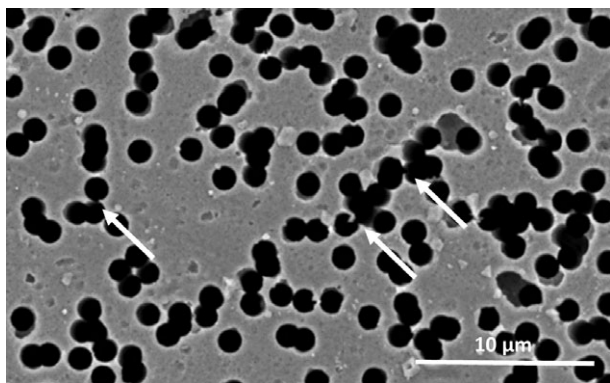


Figure 7. SEM image of a membrane after 10 times of cleaning. The white arrows show the thin walls between the pore channels that may have been affected by the high-pressure jet cleaning.

the backtransport rate of the deposited particles from the membrane. Fig. 7a shows a typical decline of the throughput due to accumulation of foulants in the membrane, as described by Kraume et al. [21]. In particular, for high-pressure jet cleaning, it is a flow that creates a wall shear stress resulting in a lifting force and a drag force to remove the adhesive particles from the wall of the pores. Burdick et al. [22] analyzed the removal of the particles on a quartz surface in a laminar flow and devel-

oped a removal criterion for particles from a surface. Based on this criterion, a minimum value of the Reynolds number can be defined for the removal of the particles. A higher pressure of the cleaning jet results in a higher velocity, a higher wall shear stress, and a higher Reynolds number [23].

As shown in Fig. 8a, the incline of the throughput of high-pressure cleaning at 130 bar is smaller than that of cleaning at 30 bar. The throughput of the membrane after cleaning at a pressure of 130 bar can be restored to up to 80 % of the initial value. Cleaning at a pressure of 130 bar results in a higher removal rate of the particles in the pores than cleaning at a pressure of 30 bar due to the higher wall shear stress.

The reduction of the pore size due to the remaining foulants can be proved by the porometer analysis of the membrane as shown in Fig. 8b. The pore size distribution of this membrane cleaned at 30 bar illustrates that the amount of the smaller pore diameters has increased significantly. The analysis of the pore size distributions matches with the throughput measurements of the membranes cleaned at 30 and 130 bar. The membrane with a higher proportion of smaller pores had a reduced throughput, whereas the membrane with a higher amount of larger pores shows a higher throughput. Although higher pressures may show a better cleaning efficiency, they were not considered, since a pressure higher than the ones chosen in this study can damage the membrane structure.

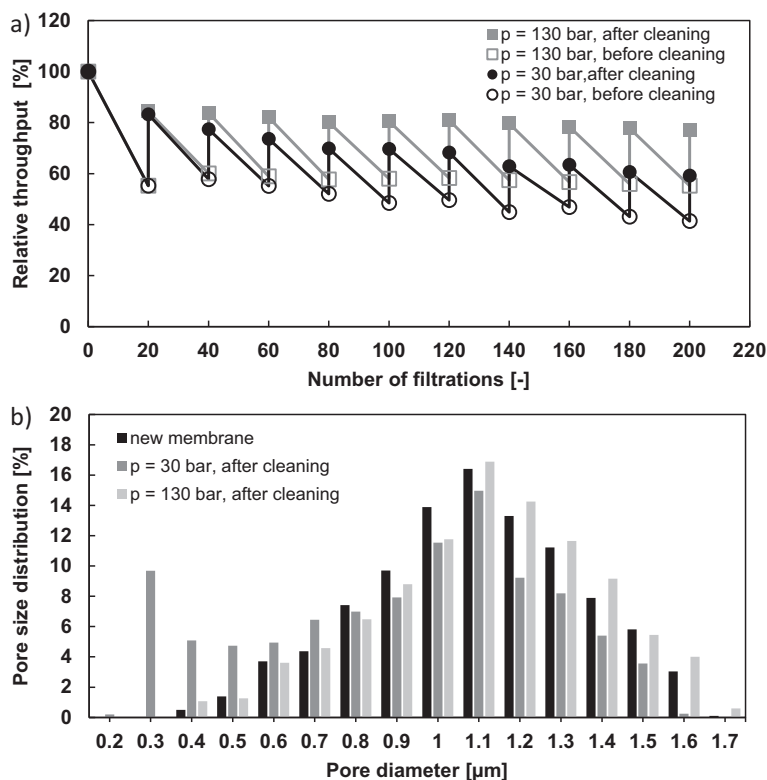


Figure 8. (a) Influence of the pressure on the throughput of the membranes (TP_{rel} at $p = 130$ bar after cleaning: 77 %; TP_{rel} at $p = 30$ bar after cleaning: 59 %). (b) Influence of the pressure on the pore size distribution of the membranes ($d = 50$ cm, $\alpha = 90^\circ$, $t = 5$ s).

3.2 Influence of the Cleaning Duration

In the following, the results of a further operation parameter are presented. The experiments in this case were carried out at a pressure of 30 bar, an angle of $\alpha = 90^\circ$, a distance of $d = 50$ cm, and at two different cleaning durations of $t = 5$ s and $t = 10$ s. As displayed in Fig. 9a, a longer duration of cleaning results in a higher throughput. The relative throughput drops to 60 % of the initial throughput at a cleaning duration of $t = 5$ s. The relative throughput continues to rise to 70 % when the cleaning duration is set at $t = 10$ s. A longer cleaning duration supports the backtransport of the adhesive particles and, as a result, the pore sizes are larger (Fig. 8b). In addition, a longer cleaning duration increases the throughput. However, longer cleaning also means higher water consumption and needs to be considered from the economic point of view.

Further experiments to investigate the most rational cleaning duration indicate that the relative throughput of the membrane did not increase after 10 s (Fig. 10). Therefore, a cleaning duration of 10 s would be suggested as realistic.

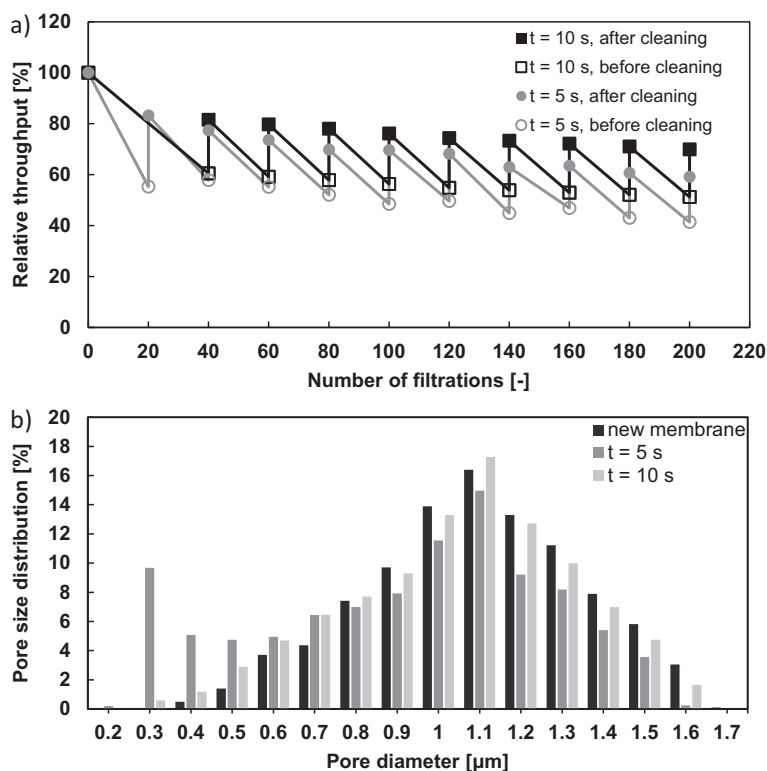


Figure 9. (a) Influence of the cleaning duration on the throughput of the membrane (TP_{rel} at $t = 10$ s after cleaning: 69%; TP_{rel} at $t = 5$ s after cleaning: 59%). (b) Influence of the cleaning duration on the pore size distribution of the membrane ($d = 50$ cm, $p = 30$ bar, $\alpha = 90^\circ$).

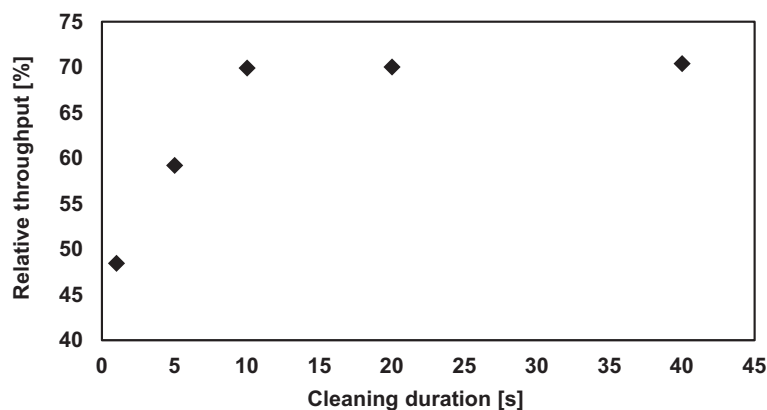


Figure 10. The relative throughput after a cleaning duration of 10 s did not show further improvements. A cleaning duration of 10 s was found to be rational ($d = 50$ cm, $p = 30$ bar, $\alpha = 90^\circ$).

3.3 Influence of the Cleaning Angle

The set of experiments described below was carried out at a pressure of 30 bar, a duration of $t = 5$ s, a distance of $d = 50$ cm, and at various angles of $\alpha = 15^\circ$, 70° , and 90° . This part investigates the influence of the angle on the high-pressure jet cleaning performance. Fig. 9a compares the throughput of the membrane after high-pressure cleaning was performed at the

different angles. The angle of 70° showed the best cleaning results and about 70 % of the initial throughput could be recovered, whereas the angle of 15° showed the lowest cleaning efficiency. The reason for this effect lies in the morphology of the membrane used in this study.

The foulants are located on the surface of the membrane and in the pore channels. To clean the foulants on the surface, flatter angles may provide a better cleaning performance due to the higher wall shear stress of the flow. Track-etched membranes show pore channels that also contain foulants. In this case, a flow in the direction of the pore can help to flush out the foulants that have accumulated in the pores during filtration. According to the criterion developed by Burdick et al. [22], an adhesive particle can be removed from the surface once the flow reaches a minimum Reynolds number. A cleaning angle that is parallel to the channel of the pore results in a higher velocity and a higher wall shear stress and may explain the higher cleaning ability. This effect explains the different pore size distributions of each operation parameter in Fig. 11b.

A CT slice of the membrane is depicted in Fig. 12a. The CT slice reveals that the pores are continuous from top to bottom and have a channel-like structure. However, the pores do not show a uniform vertical structure. The channels have various angles of declination ranging between 70° and 90° . However, most of the pore channels have declination angles between 70° and 80° . This can explain why cleaning at an angle of 70° shows a better cleaning performance than cleaning at an angle of 90° . The perpendicular flow of the jet into a 70° pore channel is deflected and, consequently, has a lower velocity and a lower wall shear stress in the pore channel. Hereby, fewer particles on the wall of the pore channels are removed, which decreases the throughput of the membrane.

As depicted in Fig. 12b, it is assumed that the fouling layer and the foulants in the upper part of the membrane are cleaned thoroughly. However, after high-pressure cleaning, some foulants still remain in the pore channels, causing a slight decline of the throughput. In the case of a low Reynolds number of the flow, it is also possible that foulants are pushed into the channel and thus clog it. Therefore, high enough Reynolds numbers are required for this mechanical cleaning method, which

is either reached by an optimal angle or a high pressure of the cleaning jet.

4 Conclusion

One main idea behind high-pressure jet cleaning was to flush out the foulants in the pores with a high-pressure jet to main-

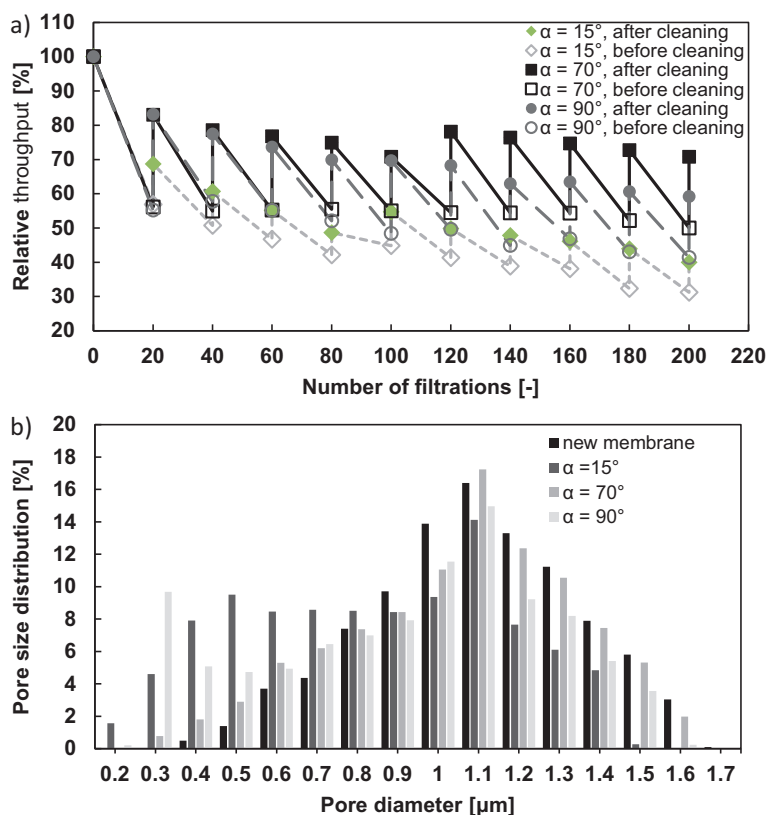


Figure 11. (a) Influence of the angle on the throughput of the membrane (TP_{rel} at $\alpha = 15^\circ$ after cleaning: 39%; TP_{rel} at $\alpha = 70^\circ$ after cleaning: 70%; TP_{rel} at $\alpha = 90^\circ$ after cleaning: 59%). (b) Influence of the angle on the pore size distribution of the membrane ($d = 50$ cm, $p = 30$ bar, $t = 5$ s).

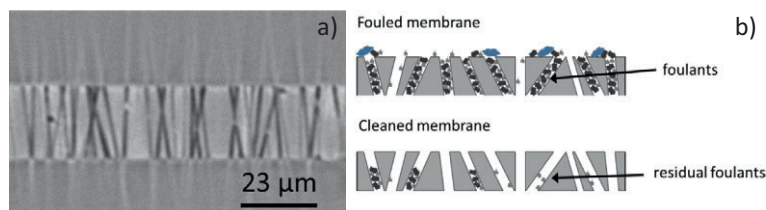


Figure 12. (a) CT image of a new membrane. (b) CT image after high-pressure jet cleaning: most foulants are removed, but some residual foulants still remain in the pores, causing a slight decrease in throughput.

tain a high throughput of the membrane. The results show that the high-pressure jet could clean most of the pores and restored up to 80% of the initial throughput of the membrane. Analysis of the pore size distributions reveals that the membranes with a lower throughput also showed a larger amount of smaller pores due to the foulants inside the pores.

For high-pressure jet cleaning, different operating parameters were compared. A higher pressure and a longer cleaning duration resulted in a higher throughput of the membrane. The higher pressure led to a higher throughput because of the higher wall shear stress, which removed the particles that adhered to the surface of the membrane and to the walls of the pore channels. Cleaning at angles of 15° and 90° results in a lower throughput compared to cleaning at an angle of

70° . The reason is that the membrane pores are not all perpendicular to the membrane surface. The CT images reveal that most of the pore channels have an incline between 70° and 80° . A direct flow parallel to the pore channel has a higher velocity and a higher wall shear stress and can therefore remove more particles.

Comparisons made between a new membrane and a membrane exposed to the high-pressure cleaning jet prove that the corresponding two pore size distributions differ only slightly. Thus, high-pressure cleaning barely affects the membrane in the defined range of operation parameters. However, after 1800 cleaning cycles, the pore size distribution of the membrane cleaned at a pressure of 130 bar shows larger pores at around $13\mu\text{m}$. This explains the results of the UV-vis analysis of the filtrate, where traces of microalgae of more than 0.01 wt% were found. It can still be concluded that high-pressure jet cleaning is an effective and promising method for the mechanical cleaning of track-etched microfiltration membranes and that it provides further options for the development of new membrane filtration processes.

Acknowledgment

The authors would like to thank M. Schmidbauer for performing parts of the experiments. The authors wish to acknowledge with sincere gratitude the financial support of the Arbeitsgemeinschaft industrieller Forschungsvereinigungen for funding of the project 18603N, which led to the publication of this article.

The authors have declared no conflict of interest.

Symbols used

A	[m ²]	filter area
d	[cm]	cleaning distance of the cleaner
p	[bar]	pressure of the jet
Δp	[bar]	gas differential pressure
Q	[L s ⁻¹]	volume flow rate
t	[s]	cleaning duration
TP	[L m ⁻² bar ⁻¹ s ⁻¹]	liquid throughput
v	[cm s ⁻¹]	speed of the lance
v_{30}	[m s ⁻¹]	flow velocity of the liquid at 30 bar
v_{130}	[m s ⁻¹]	flow velocity of the liquid at 130 bar
x	[μm]	mean pore diameter
$x_{50,3}$	[μm]	mean particle size

Greek letter

 α [°] cleaning angle

Sub- and superscripts

0 initial liquid throughput
m membrane
rel relative liquid throughput

Abbreviations

CT computed tomography
PET polyethylene terephthalate
SEM scanning electron microscopy

References

- [1] Z. Wang, J. Ma, C. Y. Tang, K. Kimura, Q. Wang, X. Han, Membrane Cleaning in Membrane Bioreactors: A Review, *J. Membr. Sci.* **2014**, *468*, 276–307. DOI: <https://doi.org/10.1016/j.memsci.2014.05.060>
- [2] F. Meng, S.-R. Chae, A. Drews, M. Kraume, H.-S. Shin, F. Yang, Recent Advances in Membrane Bioreactors (MBRs): Membrane Fouling and Membrane Material, *Water Res.* **2009**, *43* (6), 1489–1512. DOI: <https://doi.org/10.1016/j.watres.2008.12.044>
- [3] T. Tsuyuhara, Y. Hanamoto, T. Miyoshi, K. Kimura, Y. Watanabe, Influence of Membrane Properties on Physically Reversible and Irreversible Fouling in Membrane Bioreactors, *Water Sci. Technol.* **2010**, *61* (9), 2235–2240. DOI: <https://doi.org/10.2166/wst.2010.122>
- [4] C. Huyskens, S. Lenaerts, E. Brauns, L. Diels, H. De Wever, Study of (Ir)reversible Fouling in MBRs Under Various Operating Conditions Using New Online Fouling Sensor, *Sep. Purif. Technol.* **2011**, *81* (2), 208–215. DOI: <https://doi.org/10.1016/j.seppur.2011.07.031>
- [5] S. Judd, *The MBR Book: Principles and Applications of Membrane Bioreactors for Water and Wastewater Treatment*, 2nd ed., Butterworth-Heinemann, Oxford **2011**.
- [6] A. Resosudarmo, Y. Ye, P. Le-Clech, V. Chen, Analysis of UF Membrane Fouling Mechanisms Caused by Organic Interactions in Seawater, *Water Res.* **2013**, *47* (2), 911–921. DOI: <https://doi.org/10.1016/j.watres.2012.11.024>
- [7] M. Xu, X. Wen, X. Huang, Z. Yu, M. Zhu, Mechanisms of Membrane Fouling Controlled by Online Ultrasound in an Anaerobic Membrane Bioreactor for Digestion of Waste Activated Sludge, *J. Membr. Sci.* **2013**, *445*, 119–126. DOI: <https://doi.org/10.1016/j.memsci.2013.06.006>
- [8] A. L. Ahmad, N. F. C. Lah, S. Ismail, B. S. Ooi, Membrane Antifouling Methods and Alternatives: Ultrasound Approach, *Sep. Purif. Rev.* **2012**, *41* (4), 318–346. DOI: <https://doi.org/10.1080/15422119.2011.617804>
- [9] K.-K. Ng, C.-J. Wu, H.-L. Yang, C. Panchangam, Y.-C. Lin, P.-K. A. Hong, C.-H. Wu, C. F. Lin, Effect of Ultrasound on Membrane Filtration and Cleaning Operations, *Sep. Sci. Technol.* **2012**, *48* (2), 215–222. DOI: <https://doi.org/10.1080/01496395.2012.682289>
- [10] Y. Gao, D. Chen, L. K. Weavers, H. W. Walker, Ultrasonic Control of UF Membrane Fouling by Natural Waters: Effects of Calcium, pH, and Fractionated Natural Organic Matter, *J. Membr. Sci.* **2012**, *401–402*, 232–240. DOI: <https://doi.org/10.1016/j.memsci.2012.02.009>
- [11] J. Wang, X. Gao, Y. Xu, Q. Wang, Y. Zhang, X. Wang, C. Gao, Ultrasonic-Assisted Acid Cleaning of Nanofiltration Membranes Fouled by Inorganic Scales in Arsenic-Rich Brackish Water, *Desalination* **2016**, *377*, 172–177. DOI: <https://doi.org/10.1016/j.desal.2015.09.021>
- [12] T. G. Leighton, *The Acoustic Bubble*, 1st ed., Academic Press, San Diego, CA **1994**.
- [13] I. Masselin, X. Chasseray, L. Durand-Bourlier, J.-M. Lain, P.-Y. Syzarefand, D. Laemordant, Effect of Sonication on Polymeric Membranes, *J. Membr. Sci.* **2001**, *181* (2), 213–220. DOI: [https://doi.org/10.1016/S0376-7388\(00\)00534-2](https://doi.org/10.1016/S0376-7388(00)00534-2)
- [14] L. Liu, Z. Ding, L. Chang, M. Runyu, Z. Yang, Ultrasonic Enhancement of Membrane-based Deoxygenation and Simultaneous Influence on Polymeric Hollow Fiber Membrane, *Sep. Purif. Technol.* **2007**, *56* (2), 133–142. DOI: <https://doi.org/10.1016/j.seppur.2007.01.023>
- [15] M. Kallioinen, M. Mänttari, Influence of Ultrasonic Treatment on Various Membrane Materials: A Review, *Sep. Sci. Technol.* **2011**, *46* (9), 1388–1395. DOI: <https://doi.org/10.1080/01496395.2011.571649>
- [16] R.-S. Juang, K.-H. Lin, Flux Recovery in the Ultrafiltration of Suspended Solutions with Ultrasound, *J. Membr. Sci.* **2004**, *243* (1–2), 115–124. DOI: <https://doi.org/10.1016/j.memsci.2004.06.013>
- [17] H. Anlauf, A. Erk, Continuous “Skin” Filtration of Very Difficult-to-Filter Suspensions, *AT, Aufbereit. Tech.* **2006**, *47* (3), 22–29.
- [18] Z. Lam, H. Anlauf, H. Nirschl, Roller Discharge of Thin Film Filter Cakes from Membranes: A Key to the Thin Film Filtration, *Sep. Purif. Technol.* **2019**, *221*, 38–43. DOI: <https://doi.org/10.1016/j.seppur.2019.03.062>
- [19] R. Bhave, T. Kuritz, L. Powell, D. Adcock, Membrane-based Energy Efficient Dewatering of Microalgae in Biofuels Production and Recovery of Value Added Co-products, *Environ. Sci. Technol.* **2012**, *46* (10), 5599–5606. DOI: <https://doi.org/10.1021/es204107d>
- [20] F. Meng, S.-R. Chae, A. Drews, M. Kraume, H.-S. Shin, F. Yang, Recent Advances in Membrane Bioreactors (MBRs): Membrane Fouling and Membrane Material, *Water Res.* **2009**, *43* (6), 1489–1512. DOI: <https://doi.org/10.1016/j.watres.2008.12.044>
- [21] M. Kraume, D. Wedi, J. Schaller, V. Iversen, A. Drews, Fouling in MBR: What Use are Lab Investigations for Full Scale Operation?, *Desalination* **2009**, *236* (1–3), 94–103. DOI: <https://doi.org/10.1016/j.desal.2007.10.055>
- [22] G. M. Burdick, N. S. Berman, S. P. Beaudoin, Hydrodynamic Particle Removal from Surfaces, *Thin Solid Films* **2005**, *488* (1–2), 116–123. DOI: <https://doi.org/10.1016/j.tsf.2005.04.112>
- [23] W. Blel, T. Benezech, P. Legentilhomme, J. Legrand, C. Le Gentil-Lelievre, Effect of Flow Arrangement on the Removal of Bacillus Spores from Stainless Steel Equipment Surfaces During a Cleaning in Place Procedure, *Chem. Eng. Sci.* **2007**, *62* (14), 3798–3808. DOI: <https://doi.org/10.1016/j.ces.2007.04.011>